切である．血液ポンプに触れる場合，手洗いと消毒を徹底し，手袋を使用する．さらに，カニューレの皮膚貫通部に力を加えないように配慮し，同部の創傷治癒の促進を図る．また，血液ポンプの動揺が少なくなるように固定カバーを用いる．同部の発赤や発熱など感染兆候に注意し，感染対策室と連携して抗生剤の投与などを行う．

11．機器および環境の整備

VAS適用患者では，常に駆動が必要であり，定期的に装置の異常がないかチェックする．また，安定した電源と空気圧源の確保を行う．バッテリの完全充電には通常24時間以上かかり，フル充電しても，内蔵空気圧装置を用いた場合の持続時間は30分程度であり，常にバッテリをAC電源に接続しておく．

12．最後に

最大限の薬物治療やIABP，PCPSなどの補助循環を使用しても改善しない重症心不全患者がVASの対象となる．長期の使用を考慮すれば体内埋込み式が望ましいが，現在使用できる装置は大きく，体格の面で使用できない患者が多い．また，両心補助が必要な場合にも体外設置式で対応せざるを得ない．また，緊急症例では体外設置式が第一選択となる．体外設置式においても3年以上の駆動が可能であり，小型駆動装置が導入されれば病院外での生活も可能となるため，当面，体外設置式VASは必要と考えられる．

■著者連絡先メールアドレス
tnakatan@res.ncvc.go.jp

用語解説

＊1 counterpulsation
心周期に同期させて，自己心の収縮時にIABPのバルーンを収縮させる，あるいはVAS血液ポンプへの血液流入を行い，自己心の拡張時にIABPのバルーンを膨張させる，あるいはVAS血液ポンプからの拍出を行うことで，心収縮力の有効利用(systolic unloading)を行なうとともに，冠血流を増大させる(diastolic augumentation)．

＊2 PT-INR
プロトロンビン時間(PT)は，抗凝固薬として用いられるワーファリンの効果を判定するために用いられてきた．しかし，このPT値には施設間でのばらつきがあるため，PTの測定結果を標準化するために，最近ではInternational Normalized Ratio (INR：国際標準比)で表すようになった．人工弁装着患者では通常PT-INRを2～3に維持するようにワーファリンの投与が行われる．

■文　献

1) Kusserow BK: A permanently indwelling intracorporeal blood pump to substitute for cardiac function, Trans Am Soc Artif Intern Organs 4: 227, 1958
2) DeBakey ME: Left ventricular bypass pump for cardiac assistance. Clinical experience, Am J Cardiol 27: 3-11, 1971
3) 中谷武嗣: 重症心不全に対する体外設置型補助人工心臓治療－わが国の臨床経験，Heart View 3(4): 78-82, 1999
4) 中谷武嗣: 各種の補助人工心臓の種類とわが国の患者登録(補助人工心臓のABC)，ICUとCCU 25(7): 471-478, 2001
5) Takano H, Nakatani T: Ventricular assist systems: experience in Japan with Toyobo pump and Zeon pump, Ann Thorac Surg 61: 317-322, 1996
6) Farrar DJ: The thoratec ventricular assist device: a paracorporeal pump for treating acute and chronic heart failure, Semin Thorac Cardiovasc Surg 12: 243-250, 2000
7) 中谷武嗣，花谷彰久，庭屋和夫: 補助人工心臓のメインテナンス，ハートナーシング2002年秋季増刊: 228-233, 2002
8) 中谷武嗣: 補助循環と心臓移植，カレントテラピー22: 71-76, 2004
9) 平川祐子，堀由美子，奥田理恵子ほか: 補助人工心臓装着中の患者看護，ハートナーシング2002秋季増刊: 101-118, 2002

J Artif Organs (2004) 7:121–127
DOI 10.1007/s10047-004-0258-8

ORIGINAL ARTICLE

Hwansung Lee, PhD · Tomonori Tsukiya, PhD
Akihiko Homma, PhD · Tadayuki Kamimura, PhD
Yoshiaki Takewa, MD, PhD · Eisuke Tatsumi, MD, PhD
Yoshiyuki Taenaka, MD, PhD
Hisateru Takano, MD, PhD · Soichiro Kitamura, MD, PhD

Observation of cavitation bubbles in monoleaflet mechanical heart valves

Abstract Recently, cavitation on the surface of mechanical heart valves (MHVs) has been studied as a cause of fractures occurring in implanted MHVs. In the present study, we investigated the mechanism of MHV cavitation associated with the Björk–Shiley valve and the Medtronic Hall valve in an electrohydraulic total artificial heart (EHTAH). The valves were mounted in the mitral position in the EHTAH. The valve closing motion, pressure drop measurements, and cavitation capture were employed to investigate the mechanisms for cavitation in the MHV. There are no differences in valve closing velocity between the two valves, and its value ranged from 0.53 to 1.96 m/s. The magnitude of negative pressure increased with an increase in the heart rate, and the negative pressure in the Medtronic Hall valve was greater than that in the Björk–Shiley valve. Cavitation bubbles were concentrated at the edge of the valve stop; the major cause of these cavitation bubbles was determined to be the squeeze flow. The formation of cavitation bubbles depended on the valve closing velocity and the valve leaflet geometry. From the viewpoint of squeeze flow, the Björk–Shiley valve was less likely to cause blood cell damage than the Medtronic Hall valve in our EHTAH.

Key words Cavitation · Mechanical heart valve · Electrohydraulic total artificial heart

Received: December 15, 2003 / Accepted: May 31, 2004

H. Lee (✉) · T. Tsukiya · A. Homma · T. Kamimura · Y. Takewa · E. Tatsumi · Y. Taenaka · H. Takano · S. Kitamura
Department of Artificial Organs, Research Institute, National Cardiovascular Center, 5-7-1 Fujishiro-dai, Suita, Osaka 565-8565, Japan
Tel. +81-6-6833-5004 (ext. 2368); Fax +81-6-6835-5406
e-mail: hslee@ri.ncvc.go.jp

Introduction

Collapsing cavitation bubbles generate high pressure, which in turn may damage the surface of a mechanical heart valve.[1,2] The high pressure emanating from the collapsing cavities may also damage formed elements in red blood cell trauma.[3,4] Proposed mechanisms for generating sufficiently low pressure for cavitation to occur include water hammer, venturi, and squeeze flow effects.[5–7]

Lee et al.[8] and Shu et al.[9] examined the use of the experimentally measured maximum ventricular pressure slope (dp/dt) as the loading index and investigated the cavitation threshold of dp/dt for different mechanical heart valves using stroboscopic photography. However, the use of dp/dt has been questioned because of differences in the mounting and ventricular chamber compliance, and because the maximum dp/dt only occurred after valve closure.

In previous studies, we have shown that cavitation erosion on the valve surface increases with an increase in the closing velocity.[10,11] Moreover, erosion pit generation caused by cavitation was shown to be restricted to an area on the valve surface next to the edge of the valve stop where the squeeze flow had occurred. The maximum closing velocity of the leaflet contributes to the occurrence of squeeze flow. Previous work in our laboratory, using an EHTAH in an overflow mock circulatory system and using the maximum closing velocity of the leaflet, has included investigation of possible causes of cavitation in the Björk–Shiley valve, but cavitation bubbles have not been visualized.[12]

To determine the best mechanical heart valve for our EHTAH, in this initial study we investigated the mechanism for cavitation associated with the Björk–Shiley valve and the Medtronic Hall valve. It is recognized that compliance of the tube contact with the mock tester can influence MHV cavitation, but in this study, tube compliance was not modeled. Flow phenomena investigated included: the venturi effect caused by flow regurgitation during and after valve closure, the water hammer effect caused by the sudden stopping of the MHV leaflet, and squeeze flow phenomena that can take place in the narrow gap between the leaflet and the valve stop.

Fig. 1. An electrohydraulic total artificial heart connected to a mock loop tester. (*A*) Flexible tube, (*B*) actuator, (*C*) left blood pump, (*D*) acrylic chamber, (*E*) mock loop tester

In this study, to investigate the mechanism of cavitation bubble formation associated with the Medtronic Hall valve and the Björk–Shiley valve in an EHTAH, we measured three parameters. First, to investigate the mechanism for cavitation bubble formation, an image was created of the cavitation bubbles using a high-speed camera. Second, to estimate the effect of water hammer on MHV cavitation, the pressure drop in the vicinity of the valve surface was measured using a miniature pressure sensor. Then, to investigate the effect of the squeeze flow phenomenon on MHV cavitation, the closing of the valve was observed using a laser displacement sensor.

Materials and methods

The EHTAH (stroke volume: 80 ml) that was used in this study was developed by the National Cardiovascular Center in Japan (NCVC); this heart model consists of two diaphragm-type blood pumps, an actuator, and a controller (Fig. 1).[13,14] The actuator is connected to both blood pumps by a flexible tube filled with silicon oil. This EHTAH system functions as follows: silicon oil drives the blood pump via the forward and reverse rotation of the impeller. The EHTAH was connected to a mock circulatory loop tester and was run under full filling and full eject conditions.

A 25-mm Björk–Shiley valve and a Medtronic Hall valve were mounted in the mitral valve position. The blood pumps were run from 60 to 100 beats/min and the cardiac outputs ranged from 4.8 to 7.7 l/min, respectively. Regarding the pressure conditions, the pre- and after-load of the right blood pump were fixed at 10 and 30 mmHg, respectively, and the pre- and after-load of the left blood pump were fixed at 10 and 100 mmHg, respectively. Tap water at room temperature was used as the test fluid.

A CCD laser displacement sensor (LK-080, Keyence, Osaka, Japan) with a resonance frequency of 1 kHz was used to detect the closing motion of the leaflet (Fig. 2). The chamber was constructed from acrylic resin for optical access, and the laser displacement sensor was placed on top of the acrylic chamber. We used a triangulating laser light to measure leaflet motion. A piezoelectric pressure transducer (105C02, PCB Piezotronics, Depew, NY, USA) with a resonant frequency of 250 kHz was mounted approximately 10 mm from the major orifice of the mitral valve surface (Fig. 2). The mean value and standard deviation of the pressure drop and closing velocity were calculated from 30 measurements. Then, a high-speed camera (fx-6000, nac, Tokyo, Japan) was used to create an image of the cavitation bubbles (Fig. 2); the cavitation bubbles were recorded at 10000 frames per second.

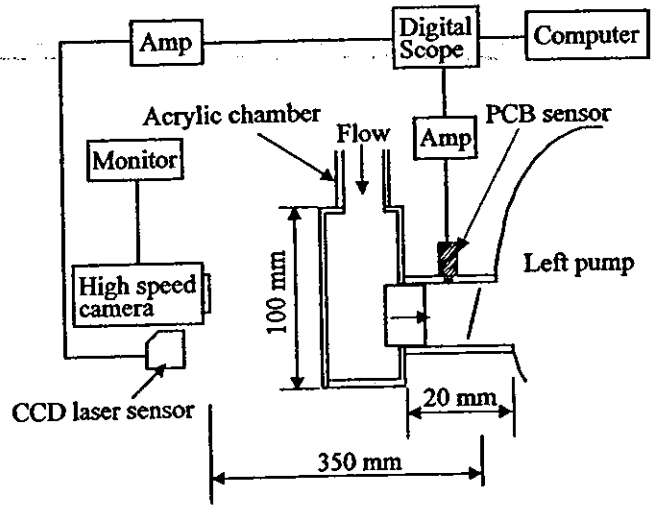

Fig. 2. High-speed camera system used for the observation of cavitation bubbles. *PCB*, piezoelectric pressure transducer

Table 1. Maximum closing velocity of the Björk–Shiley and Medtronic Hall valves

Heart rate (bpm)	Medtronic Hall valve closing velocity (m/s)	Björk–Shiley valve closing velocity (m/s)
60	0.70 ± 0.29	0.53 ± 0.14
70	1.36 ± 0.21	1.33 ± 0.11
80	1.52 ± 0.22	1.51 ± 0.19
90	1.73 ± 0.42	1.78 ± 0.18
100	1.96 ± 0.61	1.91 ± 0.24

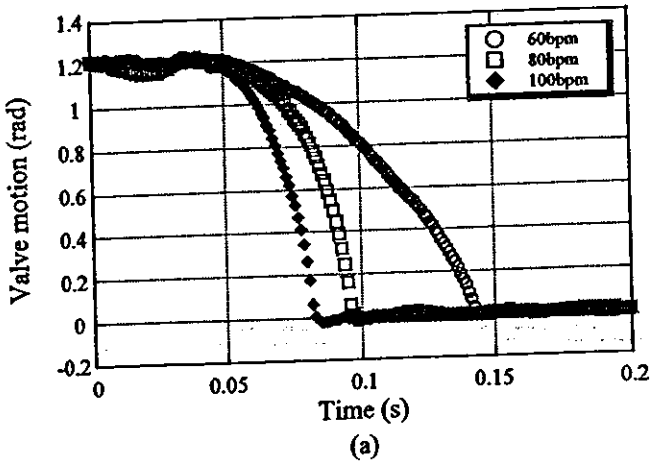

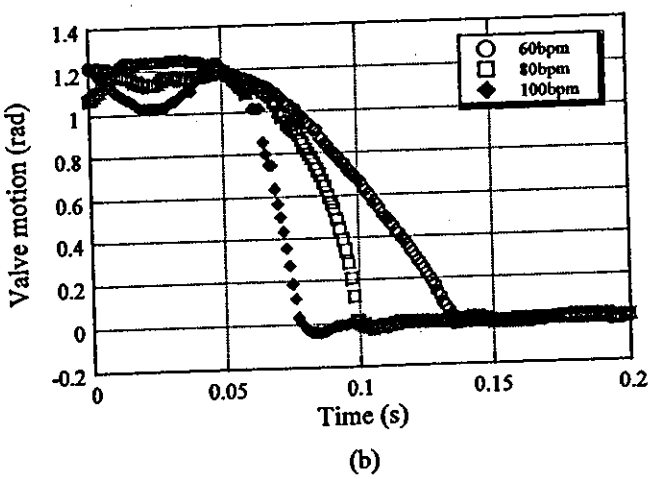

Fig. 3a,b. Closing motion of the leaflet at various heart rates. **a** Björk–Shiley valve, **b** Medtronic Hall valve

Results

The closing motions of the leaflet at various heart rates are shown in Fig. 3. In both valves, at the exact moment when the valve closed, the leaflet accelerated and reached a maximum velocity and then stopped with maximum deceleration. The closing velocity increased with an increase in the heart rate; its valve ranged from 0.53 to 1.96 m/s. There was no significant difference in the closing velocity of the leaflet between the two valves (Table 1).

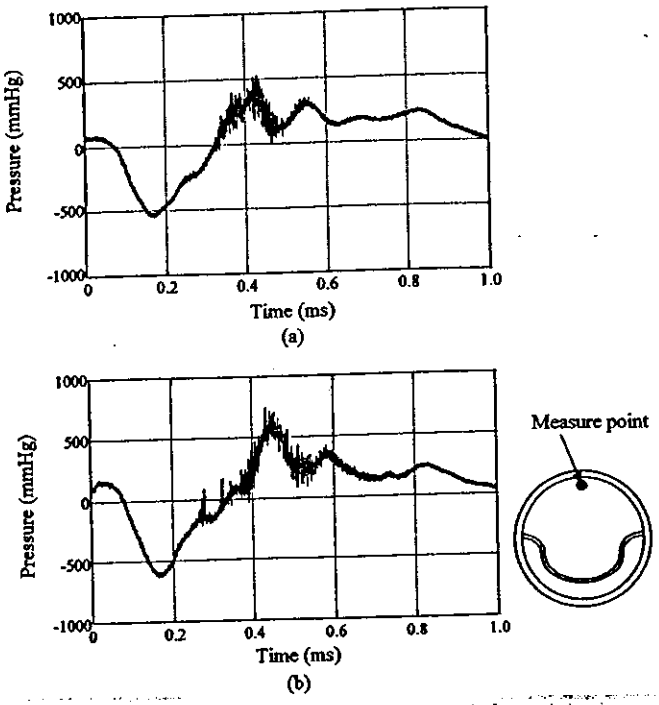

Fig. 4a,b. Pressure waveforms near the valve surface of the Björk–Shiley valve. **a** Heart rate of 80 bpm, **b** heart rate of 100 bpm

The pressure waveforms measured near the disk surface during a closing period are shown in Figs. 4 and 5. In the case of the Björk–Shiley valve, even for higher heart rates the pressure drop did not reach the critical level of more than 736 mmHg below atmospheric pressure, at which tap water at 25°C boils (Fig. 4b). In contrast, the pressure drop did reach the critical level for the higher heart rate of the Medtronic Hall valve (Fig. 5b). There were no substantial differences in the pressure waveform at various heart rates in the same valve. The magnitude of the negative pressure involutional increased with an increase in the heart rate, and the negative pressure in the Medtronic Hall valve was greater than that in the Björk–Shiley valve (Fig. 6).

Taken 200 μs after valve closure, images of the cavitation bubbles associated with the Björk–Shiley valve at different heart rates are shown in Figs. 7 and 8. The dots inside the circles are cavitation bubbles observed from the inner side of the leaflet at lower heart rates (Fig. 7a), whereas cavitation bubbles in the narrow gap between the valve and the valve housing are observed at the higher heart rate (Fig. 7b). Small cavitation bubbles were observed at the edge of the valve stop (Fig. 8). The cavitation bubbles were observed for 0.3–0.5 ms and had a diameter of up to 1.3 mm.

Taken 200 μs after valve closure, images of the cavitation bubbles associated with the Medtronic Hall valve are shown in Figs. 9 and 10. Cavitation bubbles were observed at the edge of the valve stop and on the inner side of the leaflet after valve closure (Fig. 9). After valve closure, cavitation bubbles were also observed near the center hole of the Medtronic Hall valve (Fig. 10). Cavitation bubbles

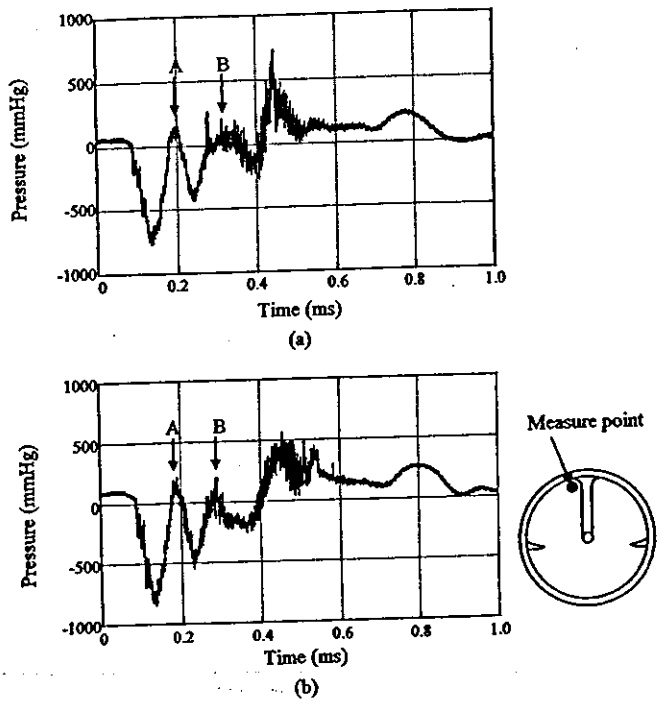

Fig. 5a,b. Pressure waveforms near the valve surface of the Medtronic Hall valve. **a** Heart rate of 80 bpm, **b** heart rate of 100 bpm. *A,B*; first and second pressure peaks

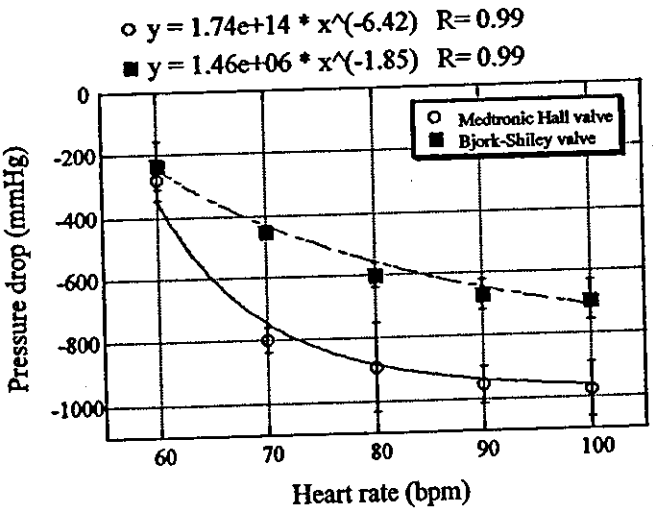

Fig. 6. Maximum negative pressure for the Björk–Shiley and Medtronic Hall valves

were observed for 0.3–0.5 ms and had a diameter of up to 0.8 mm.

In both valves, the area in which cavitation bubbles appeared and the intensity and diameter of the bubbles generally increased with an increase in the valve closing velocity, and the bubbles were observed at heart rates exceeding 70 bpm.

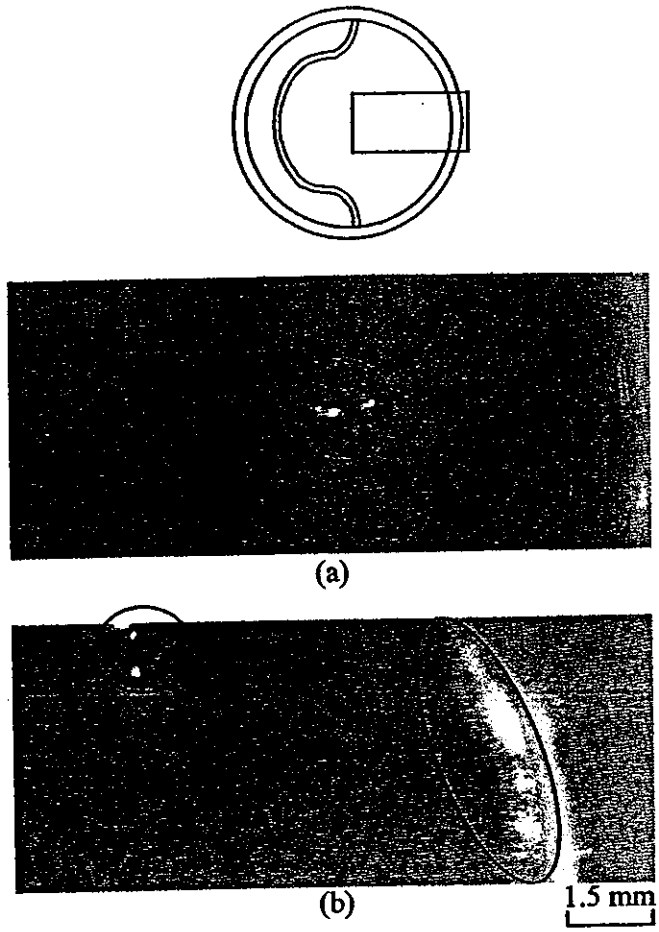

Fig. 7a,b. Images of cavitation bubbles in the Björk–Shiley valve at the major orifice 200 μs after closure. **a** Heart rate of 70 bpm, **b** heart rate of 100 bpm

Discussion

Mechanism for cavitation bubble formation

The moving fluid mass associated with the MHV closing volume tended to separate from the leaflet surface when it came to a sudden stop at closure. A negative pressure was generated with a magnitude proportional to the closing velocity and the mass of the fluid involved. This transient pressure reduction observed in the sudden closure of a leaflet is commonly known as the water hammer effect. The fluid in the gap between the leaflet and the valve stop is squeezed into motion at the moment of valve closing, and this is called squeezed flow. The squeezed flow phenomenon occurs during the final period of valve closure, in a time scale of a microsecond. The high-velocity regurgitant flows in a small gap between the valve and housing at valve closure is called the venturi effect. Even though no differences in the maximum closing velocity of the leaflet were noticed between the two types of valve (Table 1), the magnitude of the negative pressure cause by the water hammer effect in the Medtronic Hall valve was greater than that for the Björk– Shiley valve (Fig. 6). It is very likely that the

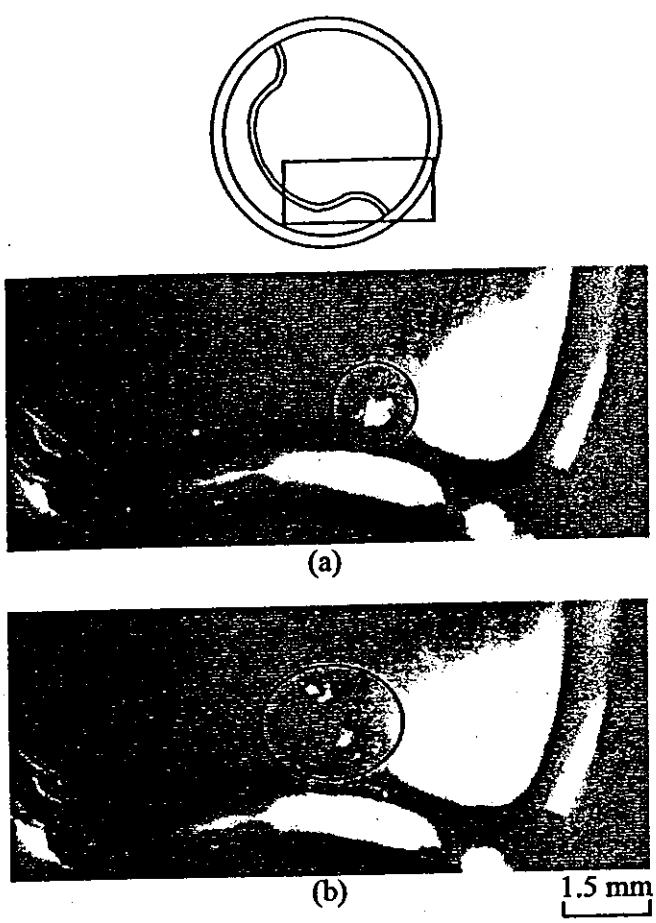

Fig. 8a,b. Images of cavitation bubbles in the Björk–Shiley valve at the valve stop 200 μs after closure. a Heart rate of 70 bmp, b heart rate of 100 bpm

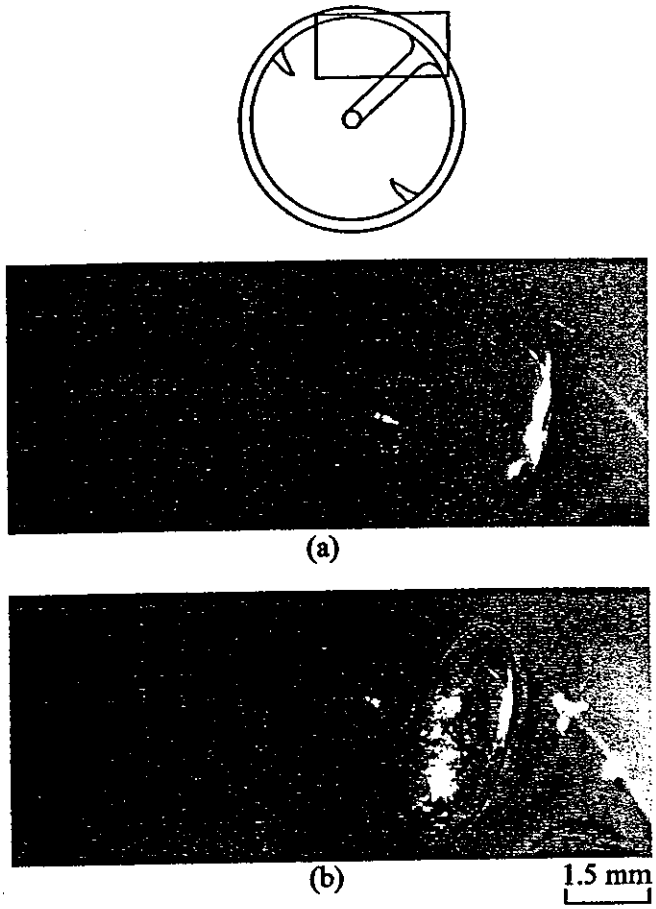

Fig. 9a,b. Images of cavitation bubbles in the Medtronic Hall valve at the major orifice 200 μs after closure. a Heart rate of 70 bpm, b heart rate of 100 bpm

large negative pressure in the Medtronic Hall valve was caused not only by water hammer but also by squeeze flow. For example, in the case of the Medtronic Hall valve, squeeze flow is generated from the valve stop just before closure of the leaflet, which causes generation of an additional pressure drop. It is also possible that the first and second positive pressure peaks (A, B in Fig. 5) were generated by reflection of the squeeze flow; the reflected flow hits the pressure sensor after valve closure because the pressure wave was measured near to the valve stop of the Medtronic Hall valve. There were no significant differences in the valve closing motion between the two valves, however, they exhibit different pressure drop waveforms. We therefore think that the differences in the pressure drop waveforms were caused not by the valve closing motion but by the valve geometry. The large magnitude of the negative pressure in the Medtronic Hall valve increased the intensity of cavitation bubbles in the Medtronic Hall valve. However, as shown in Fig. 4, even though the magnitude of negative pressure in the Björk–Shiley valve was less than that in the Medtronic Hall valve, the duration of the negative pressure in the Björk–Shiley valve was greater than that in the Medtronic Hall valve, which caused the bubbles in the Björk–Shiley valve to be of larger diameter (Figs. 7 and 8). We also observed cavitation bubbles in the narrow gap between the leaflet and the valve housing in the Björk–Shiley valve at higher heart rates (Fig. 7b) and at the center hole of the leaflet in the Medtronic Hall valve (Fig. 10b), and these bubbles were generated by venturi effects.

Position at which cavitation bubbles were generated

In the Medtronic Hall valve, most of the cavitation bubbles were generated in the region close to the inside edge of the valve stop (Fig. 9). We noticed that the size of the area in which cavitation bubbles appeared increased with an increase in the closing velocity. These results suggest that cavitation bubbles are induced by squeeze flow. In general, the squeeze flow velocity is proportional to the valve closing velocity and the area of the valve stop.

In the case of the Björk–Shiley valve, we saw small cavitation bubbles at the valve stop (Fig. 8). In the Björk–Shiley valve, the valve stop is located on the inner side of the leaflet, so the contact velocity with the valve stop was lower than the valve tip velocity. The slow closing velocity de-

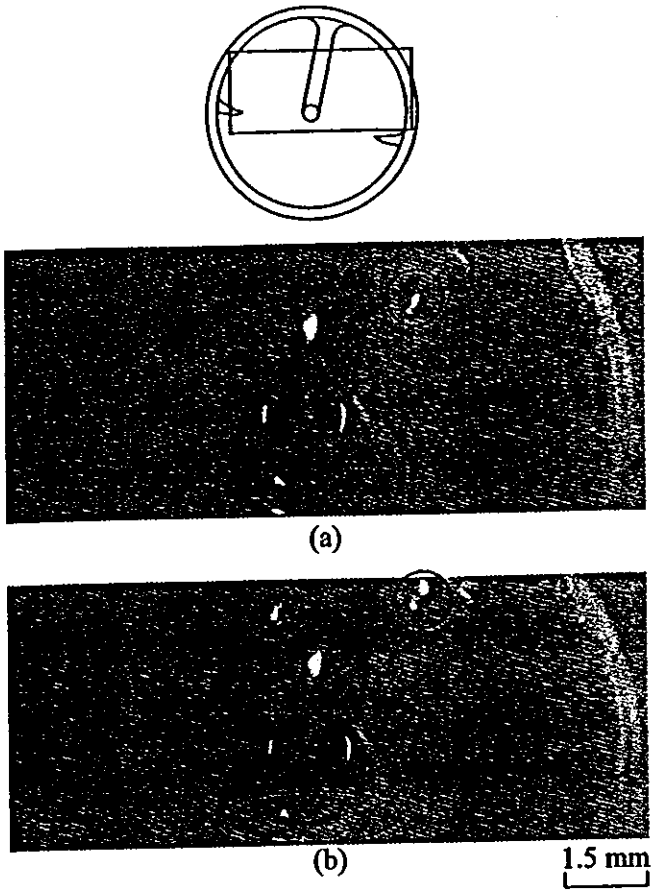

Fig. 10a,b. Images of cavitation bubbles in the Medtronic Hall valve at the inner side of the leaflet 200 μs after closure. **a** Heart rate of 70 bpm, **b** heart rate of 100 bpm

creased the intensity of cavitation bubbles at the valve stop. In general, MHV cavitation is a random phenomenon and is not repeatable, but it was dependent on the valve closing velocity. However, for the Björk–Shiley valve, the standard deviation of the closing velocity and the pressure drop was less than those for the Medtronic Hall valve.

The leaflet of the Björk–Shiley valve was designed to have a streamlined shape. The leaflet of the Medtronic Hall valve is plate shaped, and therefore a lift force causes a flutter motion during leaflet closure. At the moment of valve closure, therefore, the closing motion of the Björk–Shiley valve is more stable than that of the Medtronic Hall valve under the driving condition of our EHTAH. From the viewpoint of squeeze flow, the Björk–Shiley valve, with lower cavitation intensity at the valve stop, would presumably cause less blood cell damage than the Medtronic Hall valve in our EHTAH.

Although cavitation phenomena in MHVs differ depending on the working fluid, the results of this study provide useful information on the selection of a suitable MHV in an EHTAH system.

Conclusions

In the case of the Medtronic Hall valve, most cavitation bubbles were observed in the present study at the edge of the valve stop; the major cause of these cavitation bubbles was determined to be the squeeze flow. In contrast, with the Björk–Shiley valve, most of the cavitation bubbles were observed on the inner side of the leaflet and were caused by water hammer. The formation of cavitation bubbles dependeds on both the valve closing velocity and the valve leaflet geometry. From our results, the Björk–Shiley valve was supposed to cause less blood cell damage than the Medtronic Hall valve in our EHTAH.

Acknowledgments This work was supported by the Foundation for Translational Research and the New Energy and Industrial Technology Development Organization.

References

1. Klepetko W, Moritz A, Mlczoch J, Schurawitzki H, Domanig E, Wolner E. Leaflet fracture in Edward–Duromedics bileaflet valves. J Thorac Cardiovasc Surg 1989;97:90–94
2. Kafesjian R, Howanec M, Ward GD, Diep L, Wagstaff LS, Rhee R. Cavitation damage of pyrolytic carbon in mechanical heart valves. J Heart Valve Dis 1994;3(Suppl I):S2–S7
3. Graf T, Reul H, Dietz W, Wilmes R, Rau G. Cavitation at mechanical heart valves under simulated physiological conditions. J Heart Valve Dis 1992;1(1):131–141
4. Garrison LA, Lamson TC, Deutsch S, Geselowitz DB, Gaumond RP, Tarbell JM. An in-vitro investigation of prosthetic heart valve cavitation in blood. J Heart Valve Dis 1994;3(Suppl I):S8–S24
5. Wu ZJ, Wang Y, Hwang NHC. Occluder closing behavior. A key factor in mechanical heart valve cavitation. J Heart Valve Dis 1994; 3(Suppl I):S25–S34
6. Makhijani VB, Yang HQ, Singhal AK, Hwang NHC. An experimental–computational analysis of MHV cavitation: Effects of leaflet squeezing and rebound. J Heart Valve Dis 1994;3(Suppl I):S35–S48
7. Graf T, Reul H, Detlefs C, Wilmes R, Rau G. Causes and formation of cavitation in mechanical heart valve. J Heart Valve Dis 1994;3(Suppl I):S49–S64
8. Lee CS, Chandran KB, Chen LD. Cavitation dynamics of mechanical heart valve prostheses. Artif Organ 1994;18:758–767
9. Shu MCS, Leuer LH, Armitage TL, Schneider TE, Christiansen DR. In vitro observations of mechanical heart valve cavitation. J Heart Valve Disease 1994;3(Suppl I):S85–S93
10. Lee HS, Shimooka T, Mitamura Y, Yamamoto K, Yuhta T. Surface pitting of heart valve disks tested in an accelerated fatigue tester. Front Med Biol Eng 2000;10:167–176
11. Lee HS, Yamamoto K, Kudo N, Shimooka T, Mitamura Y, Yuhta T. Examination of cavitation-induced surface erosion pitting of a mechanical heart valve using closing velocities. J Artif Organs 2002;5:193–199
12. Lee HS, Tsukiya T, Homma A, Taenaka Y, Tatsumi E, Takano H. Measurement of the closing behavior of the Björk–Shiley monoleaflet mechanical heart valve with an electrohydraulic total artificial heart. Artif Organs 2003;27:744–748
13. Tatsumi E, Taenaka Y, Homma A, Nishinaka T, Takewa Y, Tsukiya T, Ohnishi H, Shirakawa Y, Kakuta Y, Shioya K, Katagiri N, Mizuno T, Kamimura T, Takano H, Tsukahara K, Tsuchimoto K, Wakui H, Yamaguchi H. The national cardiovascular center electrohydraulic total artificial heart and ventricular assist device systems: Current status of development, ASAIO J 2003;49:243–249

14. Tatsumi E, Taenaka Y, Uesho K, Homma A, Nishinaka T, Kakuta Y, Tsukiya T, Takano H, Masuzawa T, Nakamura M, Koshiji K, Fukui Y, Tsukahara K, Tsuchimoto K, Wakui H. Current status of development and in vivo evaluation of the national cardiovascular center electrohydraulic total artificial heart system. J Artif Organs 2000;3:62–69

Observation of Cavitation in a Mechanical Heart Valve in a Total Artificial Heart

Hwansung Lee, Tomonori Tsukiya, Akihiko Homma, Tadayuki Kamimura, Yoshiaki Takewa, Tomohiro Nishinaka, Eisuke Tatsumi, Yoshiyuki Taenaka, Hisateru Takano, Soichiro Kitamura

Recently, cavitation on the surface of mechanical heart valves has been studied as a cause of fractures occurring in implanted mechanical heart valves. The cause of cavitation in mechanical heart valves was investigated using the 25 mm Medtronic Hall valve and the 23 mm Omnicarbon valve. Closing of these valves in the mitral position was simulated in an electrohydraulic totally artificial heart. Tests were conducted under physiologic pressures at heart rates from 60 to 100 beats per minute with cardiac outputs from 4.8 to 7.7 L/min. The disk closing motion was measured by a laser displacement sensor. A high-speed video camera was used to observe the cavitation bubbles in the mechanical heart valves. The maximum closing velocity of the Omnicarbon valve was faster than that of the Medtronic Hall valve. In both valves, the closing velocity of the leaflet, used as the cavitation threshold, was approximately 1.3–1.5 m/s. In the case of the Medtronic Hall valve, cavitation bubbles were generated by the squeeze flow and by the effects of the venturi and the water hammer. With the Omnicarbon valve, the cavitation bubbles were generated by the squeeze flow and the water hammer. The mechanism leading to the development of cavitation bubbles depended on the valve closing velocity and the valve stop geometry. Most of the cavitation bubbles were observed around the valve stop and were generated by the squeeze flow. *ASAIO Journal* 2004; 50:205–210.

In cases involving a single mechanical heart valve, the clinical findings reported to date have indicated that pitting and erosion occur on valve leaflets.[1] Before impact, fluid contained in the gap between the housing and the approaching leaflet is squeezed out, which results in a local pressure drop. If the pressure drop falls below the vapor pressure of the liquid, cavitation bubbles will occur.[2] When cavitation bubbles flow onward into a higher pressure region, the rapid collapse of these bubbles may generate a high speed microjet and shock waves. The collapsing cavitation bubbles generate high pressures. If the bubbles collapse near the material surface, they may damage the surface of mechanical heart valves.[3]

Proposed mechanisms of generating the low pressures necessary for cavitation to occur include water hammer, venturi, and squeeze flow effects. Water hammer and squeeze flow phenomena depend on the leaflet velocity just before closure.

Graf *et al.* measured the critical disk closing velocity that induces cavitation and focused primarily on the pressure drop caused by the deceleration of a disk.[4] Lee *et al.* and Shu *et al.* examined the cavitation threshold of dp/dt for different mechanical heart valves using stroboscopic photography.[5,6] He *et al.* investigated the mechanism of the formation of cavitation bubbles in cases involving Medtronic Hall valves; in that study, the average value of the increase in the rate of transvalvular pressure was used as an index loading rate.[7] However, the gradient of the ventricular pressure differed according to ventricular chamber compliance. In previous studies, the au-

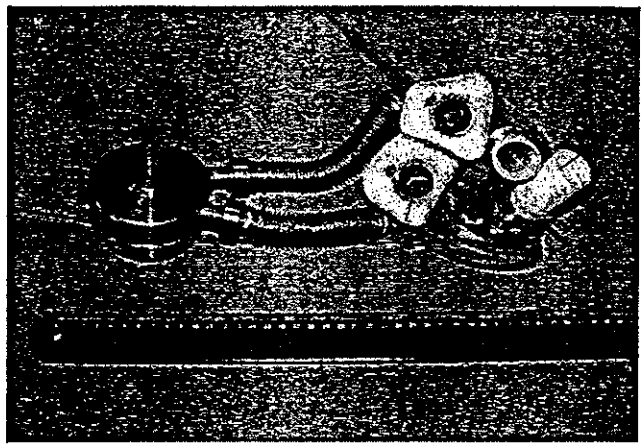

Figure 1. An electrohydraulic total artificial heart.

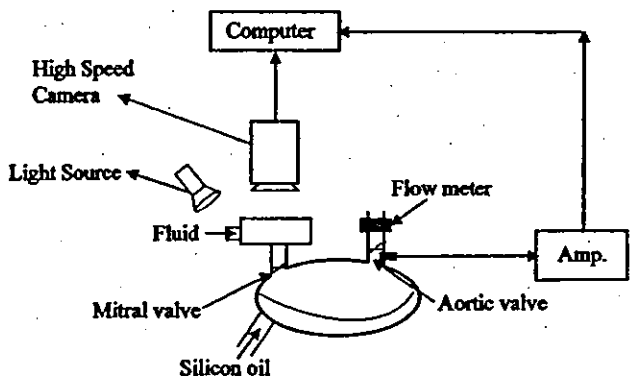

Figure 2. High speed camera system used for the observation of cavitation bubbles.

Department of Artificial Organs, Research Institute, National Cardiovascular Center, 5-7-1 Fujishiro-dai, Suita, Osaka 565-8565, Japan

Submitted for consideration July 2003, accepted in revised form January 2004.

Correspondence: Dr. H.S. Lee, Department of Artificial Organs, Research Institute, National Cardiovascular Center, 5-7-1, Fujishiro-dai, Suita, Osaka 565-8565, Japan.

DOI: 10.1097/01.MAT.0000123639.59051.C9

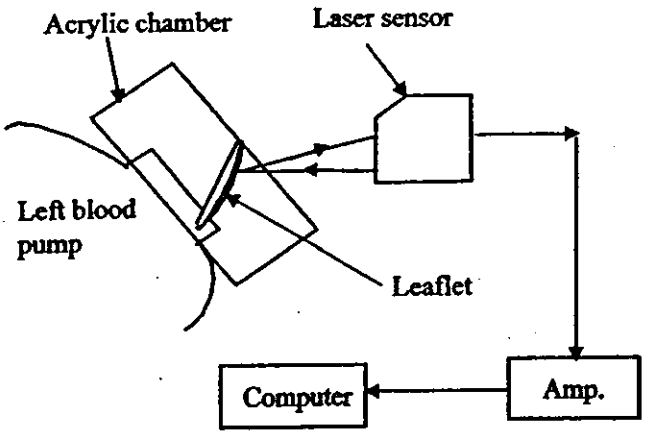

Figure 3. Laser sensor system used for the measurement of valve closing motion.

thors have shown that cavitation erosion on the valve surface increases with an increase in the closing velocity.[8] Moreover, erosion pit generation caused by cavitation was shown to be restricted to an area on the valve surface next to the edge of the valve stop where the squeeze flow had occurred. Because it is known that the maximum closing velocity of the leaflet contributes to the occurrence of squeeze flow, this velocity was used as an index of the cavitation threshold in the current study.

To investigate the mechanism of cavitation associated with the Medtronic Hall valve and the Omnicarbon valve in an electrohydraulic total artificial heart, two parameters were measured. First, an image was created of the cavitation bubbles using a high-speed camera. Next, the closing of the valve was observed using a laser displacement sensor.

Materials and Methods

The electrohydraulic total artificial heart (stroke volume 75 mL) used in this study was developed by the National Cardiovascular Center in Japan; this heart model consists of two diaphragm type blood pumps, an actuator, and a controller (**Figure 1**). The actuator is connected to both blood pumps by a flexible tube. The flexible tubes are filled with silicon oil. This electrohydraulic total artificial heart system functions as follows: silicon oil drives the blood pump via the inverse or reverse rotation of the impeller. The electrohydraulic total artificial heart used in this study was connected to an overflow mock circulatory loop tester.

A 25 mm Medtronic Hall valve and a 23 mm Omnicarbon valve were mounted in the mitral position. The leaflet diameter of the two valves was 20 and 18 mm, and the opening angle of those valves was 70° and 68°, respectively. Throughout the experiments, the 23 mm Medtronic Hall valve was mounted in the aortic position. The blood pumps were run at a heart rate from 60 to 100 beats per minute (bpm), and the cardiac outputs ranged from 4.8 to 7.7 L/min, respectively. Regarding the pressure conditions, the preload and afterload of the right blood pump was fixed at 10 and 30 mm Hg, respectively. However, the preload and afterload of the left blood pump were fixed at 10 and 100 mm Hg, respectively. Room temperature tap water was used as a test fluid.

To create an image of the cavitation bubbles, a high-speed camera (Memrecam fx 6000, nac, Tokyo, Japan) was used (**Figure 2**). The chamber was constructed from acrylic resin for optical access, and the high-speed camera was placed on top of the acrylic chamber; the cavitation bubbles were recorded at 10,000 frames per second.

A CCD laser displacement sensor (LK-080, Keyence, Corp., Tokyo, Japan) with a resonance frequency of 1 kHz was used

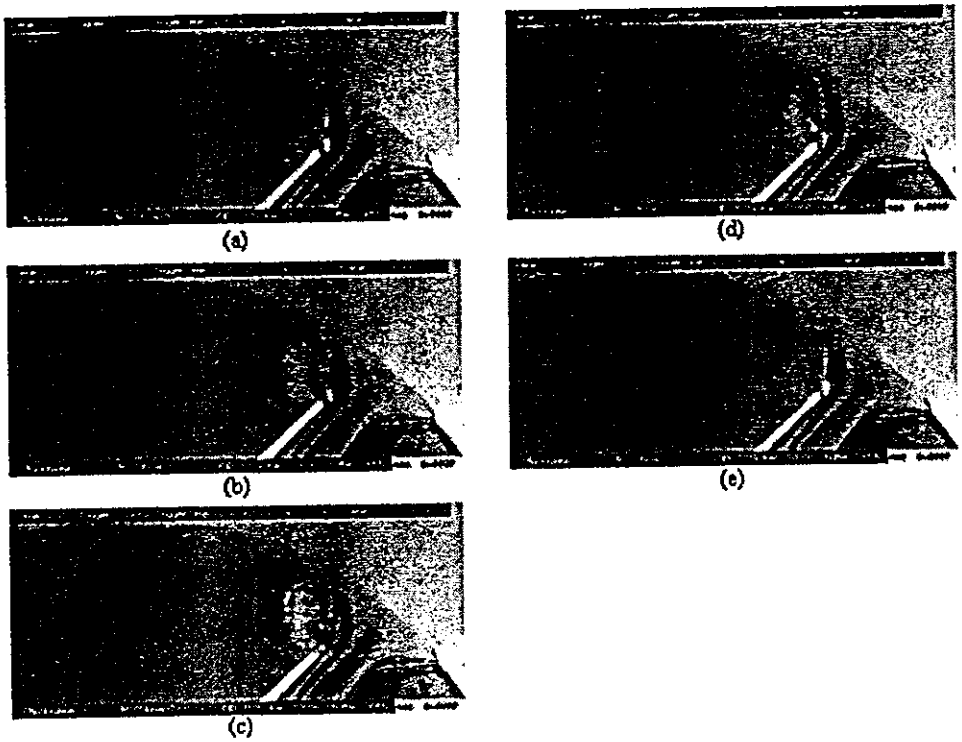

Figure 4. Cavitation bubbles in the Medtronic Hall valve (70 bpm, 10,000 frames per second): (a) contact, (b) 100 μs after contact, (c) 200 μs after contact, (d) 300 μs after contact, (e) 400 μs after contact.

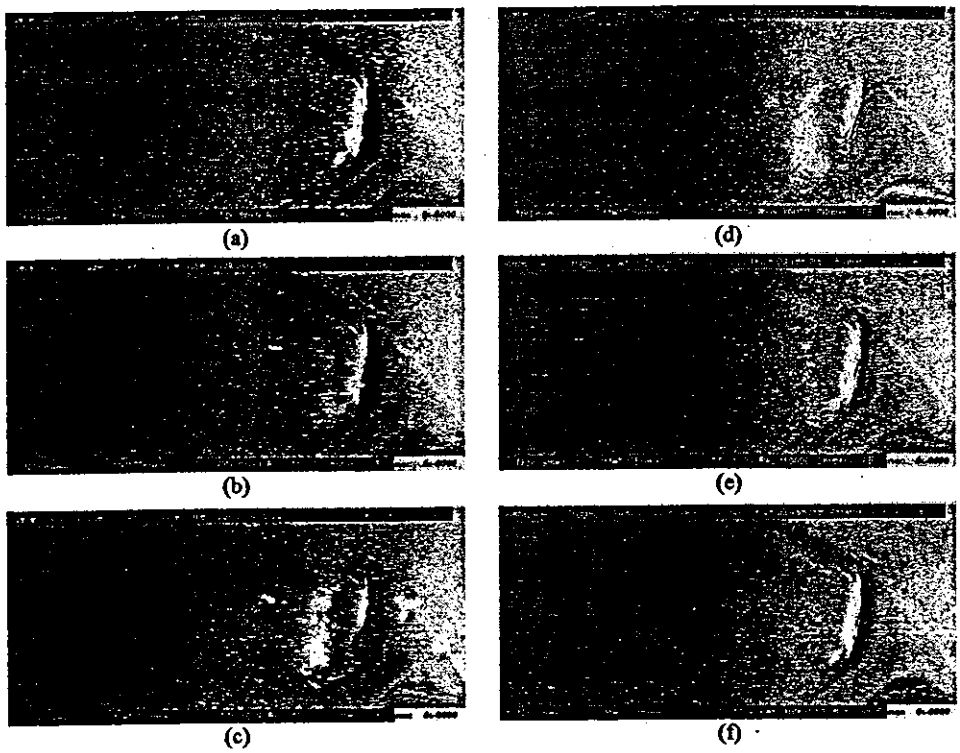

Figure 5. Cavitation bubbles in the Medtronic Hall valve (100 bpm, 10,000 frames per second): (a) contact, (b) 100 μs after contact, (c) 200 μs after contact, (d) 300 μs after contact, (e) 400 μs after contact, (f) 500 μs after contact.

to measure the opening and closing behavior of the leaflet (**Figure 3**). The laser sensor was placed on top of the acrylic chamber. To measure leaflet motion, a triangulating laser light method was used. To measure the flow rate, an electromagnetic flow meter (FR-130T, Nihon kouden, Tokyo, Japan) was positioned on the outflow side.

Results

The photographs of the cavitation bubbles associated with use of the Medtronic Hall valve are shown with the heart rate data in **Figures 4 and 5.** The duration of the interval between images was 100 μs, and the heart rate was 70 bpm. The cavitation bubbles were observed from the edge of the valve stop after the valve had closed. Cavitation bubbles were generated by the squeeze flow between the valve and the valve stop. When the heart rate reached 100 bpm, cavitation bubbles were observed in the following locations: at the edge of the valve stop, in the narrow gap between the valve and the valve housing, and on the inner side of the leaflet. The bubbles were generated by the squeeze flow, the venturi effect, and the water hammer effect, respectively. The cavitation bubbles were observed for duration of 400–500 μs.

Photographs of the cavitation bubbles associated with the Omnicarbon valve are shown in **Figures 6 and 7.** When the heart rate was 70 bpm, cavitation bubbles were observed near the edge of the valve stop. However, when the heart rate reached 100 bpm, cavitation bubbles were observed near the edge of the valve stop as well as on the inner side of the leaflet. The bubbles were generated by squeeze flow and water hammer effect. These cavitation bubbles were observed in intervals of 200–400 μs. This duration was shorter than the corresponding duration associated with the Medtronic Hall valve.

With both valves, the area in which cavitation bubbles appeared and the intensity and size of the bubbles generally increased with an increase in the valve closing velocity; in both cases, cavitation bubbles were observed at heart rates exceeding 70 bpm.

The closing of the Medtronic Hall and Omnicarbon valves is shown in **Figures 8 and 9.** The vertical axis represents the opening motion of the leaflet, and the radians reflect the closing motion of the leaflet. The vertical axis also represents the opening angle of the leaflet. For example, 1.2 on the vertical axis reflects an open state, and 0 represents a closed state. At the exact moment when the valve closed, the leaflet accelerated and reached a maximum velocity. In both valves, the closing duration decreased with a decrease in the heart rate.

The maximum closing velocity for each valve is shown in **Figure 10.** The maximum closing velocity of the Omnicarbon valve was faster than that of the Medtronic Hall valve. The maximum closing velocity of the two valves ranged from 0.78 to 2.2 m/s. Furthermore, it was found that this velocity increased with an increase in the heart rate. As indicated, the error bars were obtained from 20 measurements.

Discussion

The mechanism leading to the development of cavitation bubbles differed according to the geometry of the valve stop and the closing velocity. As shown in **Figure 11,** there is no narrow gap between the leaflet and the valve housing in the case of the Omnicarbon valve, and, therefore, no cavitation bubbles were created by the venturi effect. Cavitation bubbles were observed from the edge of the valve stop, on the inner side of the leaflet, and in the narrow gap between the leaflet and the valve housing. However, most of the cavitation bub-

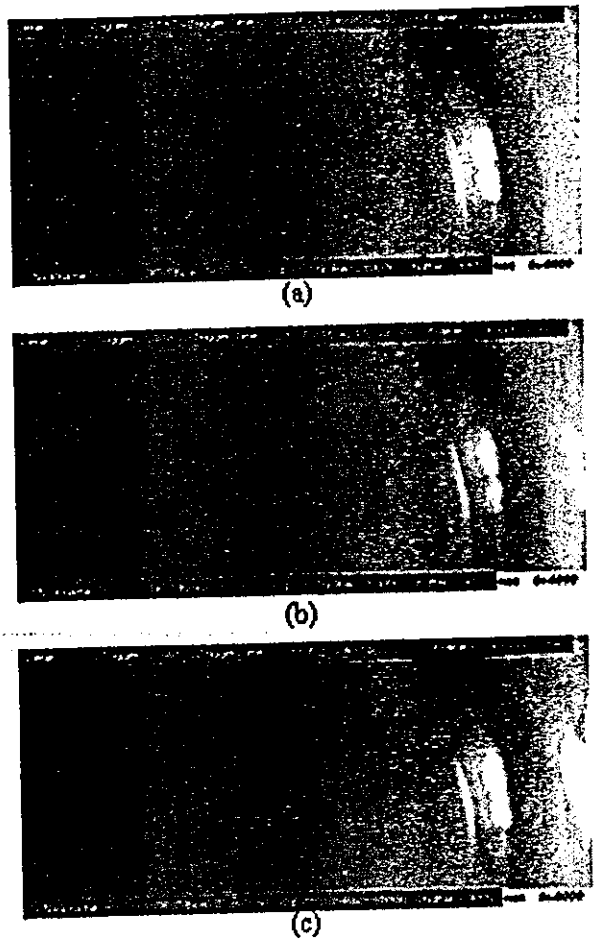

Figure 6. Cavitation bubbles in the Omnicarbon valve (70 bpm, 10,000 frames per second): (a) contact, (b) 100 μs after contact, (c) 200 μs after contact.

bles were generated in a region close to the inside edge of the valve stop. It also was observed that the area in which cavitation bubbles appeared increased with an increase in the closing velocity and the valve stop area. These results furthermore suggest that cavitation bubbles are induced by squeeze flow.

In previous studies, it was assumed that the squeeze flow, which occurs just before valve closure, leads to the pressure drop that supports cavitation formation.[8,9] A simple mechanism that accounts for the occurrence of the squeeze flow is shown in **Figure 12.** Assuming the valve closed with the maximum closing velocity and in a uniform flow from the gap, the following simple equation can be solved with respect to squeeze flow velocity U:

$$U(0) = \frac{VL}{b} = \frac{L\,db}{b\,dt}, \tag{1}$$

where b is the gap between the valve and the valve stop when a squeeze flow is generated, L is half of the length of the valve stop, and V is the valve closing velocity, and t is time. As shown in **Equation 1,** the squeeze flow velocity increases with an increase in the valve closing velocity and the valve stop area. As shown in **Figure 11,** the valve stop area (dot line of **Figure 11**)of the Medtronic Hall valve is greater than that of the Omnicarbon valve, such that there were more cavitation bubbles generated with the Medtronic Hall valve.

As shown in **Figure 11,** when the squeeze flow was emitted through gap size b, Rajaratnam reported the jet flow $U_{m(x)}$ as follows:[10]

$$\frac{U_m(x)}{U(0)} = \frac{3.5}{\sqrt{\frac{x}{b}}}, \tag{2}$$

where x is the distance from the valve stop. As can be seen in

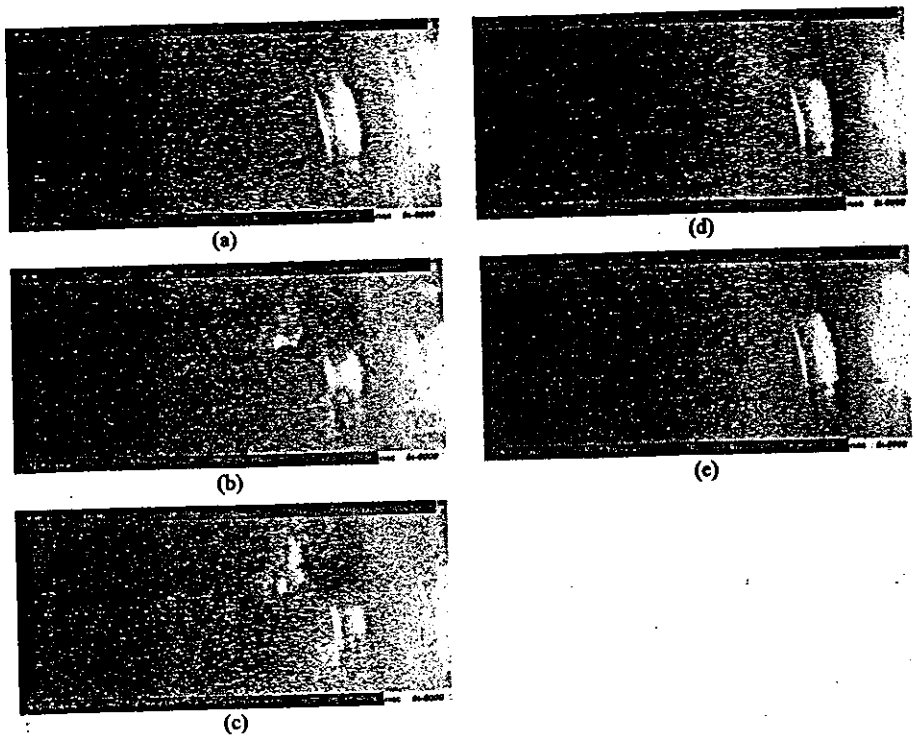

Figure 7. Cavitation bubbles in the Omnicarbon valve (100 bpm, 10,000 frames per second): (a) contact, (b) 100 μs after contact, (c) 200 μs after contact, (d) 300 μs after contact, (e) 400 μs after contact.

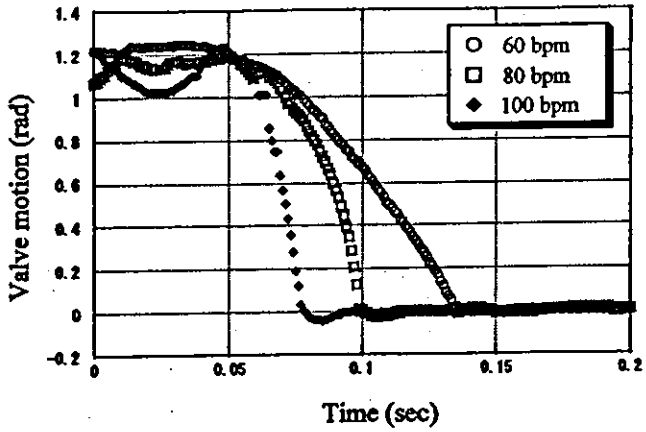

Figure 8. Closing motion of the Medtronic Hall valve. bpm, beats per minute; rad, opening angle.

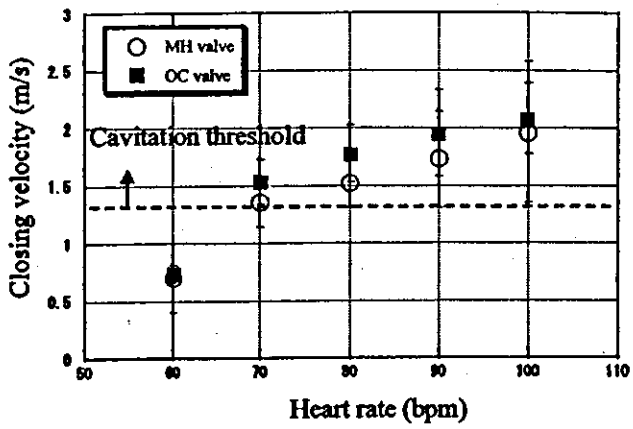

Figure 10. Maximum valve closing velocity. bpm, beats per minute.

Equation 2, the jet flow velocity $U_{m(x)}$ is directly proportional to , and, therefore, **Equation 2** may be altered to read as follows:

$$x = b\left\{\frac{3.5}{U_m(x)}\frac{VL}{b}\right\}^2, \qquad (3)$$

When the flow velocity $U_{m(x)}$ exceeds 14 m/s, the pressure falls to a critical level. This flow velocity is widely used in the field of cavitation engineering as a critical fluid velocity at which cavitation bubbles may be generated. If it is assumed that a 14 m/s insert in $U_{m(x)}$ of **Equation 3**, x can be defined as the cavitation bubble generation area. As shown in **Figures 4–7**, the cavitation bubble generation area increased with an increase in the valve closing velocity and the valve stop area. For example, as shown in **Figures 4 and 5**, x of the cavitation bubbles generation area are 0.7 mm and 1.2 mm in the Medtronic Hall valve. If those values are inserted in **Equation 3**, and the gap sizes are 120 μm and 300 μm, however, its gap size is larger than that of other group results.[11] The authors think that the squeeze flow is generated just before leaflet closure. In the future, it will be necessary to investigate gap size induced by the squeeze flow and the squeeze flow velocity induced by the occurrence of cavitation bubbles in this experimental system.

These results also suggest that cavitation bubbles are induced by squeeze flow. As shown in **Figure 11**, the valve stop area of the Medtronic Hall valve was greater than that of the Omnicarbon valve, which led to an increase in the presence of cavitation bubbles observed in association with the Medtronic Hall valve. However, there was an unknown b of gap size in this study.

In particular, cavitation bubbles caused by the water hammer effect were observed only at high speed leaflet closing velocities. However, in the case of both valves, cavitation bubbles were observed at the edge of the valve stop at heart rates exceeding 70 bpm, as shown in **Figure 10**; thus the maximum closing velocity, approximately 1.3–1.5 m/s, could be considered as the cavitation threshold. With regard to the cavitation threshold, the squeeze flow is a very important parameter. In the future, it will be necessary to investigate the squeeze flow velocity induced by the occurrence of cavitation bubbles.

Cavitation phenomenon in mechanical heart valves differ depending on the working fluid. Because the purpose of this study was to select the best mechanical heart valves for the totally artificial heart, this comparison of the cavitation mech-

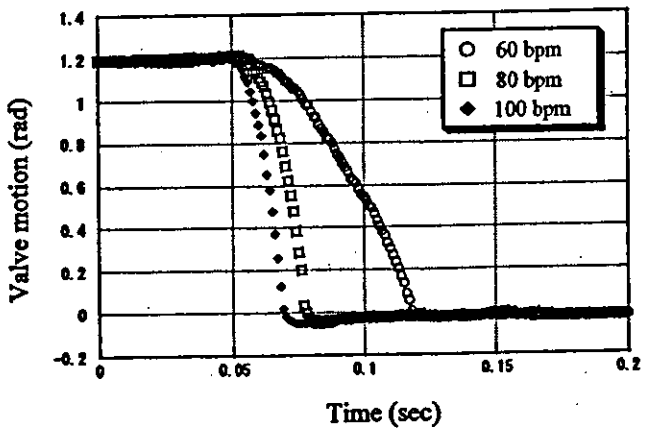

Figure 9. Closing motion of the Omnicarbon valve. bpm, beats per minute; rad, opening angle..

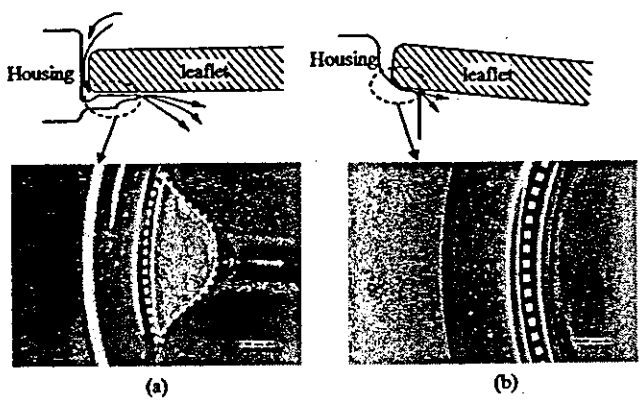

Figure 11. Configuration of the valve stop: (a) Medtronic Hall valve, (b) Omnicarbon valve.

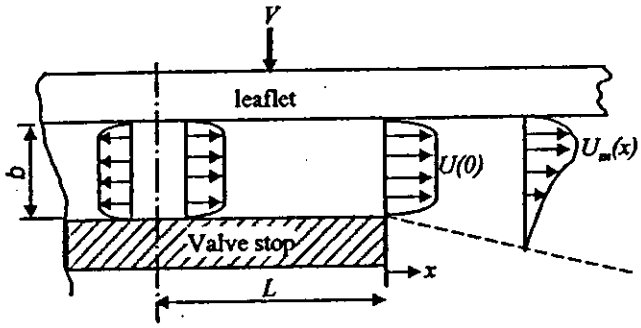

Figure 12. Mechanism for the occurrence of squeeze flow. V, valve closing velocity; U, squeeze flow velocity; $U_m(x)$, jet flow velocity.

anisms in the different mechanical heart valves appears to be valid. With regard to the cavitation threshold, the closing velocity of the leaflet is a very important parameter. From the viewpoint of squeeze flow and given the same closing velocity of the leaflet, a small size of valve stop could minimize cavitation. Even if the serious driving condition in the artificial heart, cavitation could occur when using monoleaflet valves in a clinical study.

Conclusions

Most cavitation bubbles were observed in the current study at the edge of the valve stop. The major cause of these cavitation bubbles was determined to be the squeeze flow. The formation of cavitation bubbles depended on both the valve closing velocity and the valve stop geometry. The maximum closing velocity of the Omnicarbon valve was faster than that of the Medtronic Hall valve. However, with both valves, a closing velocity of approximately 1.3–1.5 m/s could be considered as the cavitation threshold.

Acknowledgment

This work is supported by the Foundation for Translational Research of Health and Labour Science Research Grant in Japan, as well as by the New Energy and Industrial Technology Development Organization and Grant in Aid for Scientific Research of JSPS (Japan Society for the Promotion of Science).

References

1. Klepetko W, Moritz A, Mlczoch J, Schurawitzki H, Domanig E, Wolner E: Leaflet fracture in Edwards–Duromedics bileaflet valves. *J Thorac Cardiovasc Surg* 97: 90–94, 1989.
2. Knapp RT, Daily JW, Hammitt FG: *Cavitation*. Iowa City: Institute of Hydraulic Research, University of Iowa, 1979.
3. Bokros JC, LaGrange LD, Schoen FJ: Control of structure of carbon for use in bioengineering, in Walker PL (ed), *Chemistry and Physics of Carbon*. Dekker, New York, NY, 1972, pp. 103–171.
4. Graf T, Reul H, Detlefs C, Wilmes R, Rau G: Causes and formation of cavitation in mechanical heart valve. J Heart Valve Dis 3(Suppl. I): S49–64, 1994.
5. Lee CS, Chandran KB, Chen LD: Cavitation dynamics of mechanical heart valve prostheses. Artif Organs 18: 758–767, 1994.
6. Shu MCS, Leuer LH, Armitage TL, Schneider TE, Christiansen DR: *In vitro* observations of mechanical heart valve cavitation. *J Heart Valve Dis* 3(Suppl. I): S85–93, 1994.
7. He Z, Xi B, Zhu K, Hwang NHC: Mechanisms of mechanical heart valve cavitation: Investigation using a tilting disk valve model. *J Heart Valve Dis* 10: 666–674, 2001.
8. Lee HS, Shimooka T, Mitamura Y, Yamamoto K, Yuhta T: Surface pitting of heart valve disks tested in an accelerated fatigue tester. *Front Med Biol Eng* 10: 167–176, 2000.
9. Lee HS, Tsukiya T, Homma A, et al: Closing behavior of the mechanical heart valve in a total artificial heart. *The Japanese Society for Artificial Organs* 6: 37–41, 2003.
10. Rajaratnam N: *Turbulent Jets*. Amsterdam: Elsevier Scientific Publishing Company, 1976.
11. Makhijani VB, Yang HQ, Singhal AK, Hwang NHC: An experimental-computational analysis of MHV cavitation: Effect of leaflet squeezing and rebound. *J Heart Valve Dis* 3(Suppl. I): S35–48, 1994.

A Study on the Mechanism for Cavitation in the Mechanical Heart Valves with an Electrohydraulic Total Artificial Heart*

Hwansung LEE**,***, Tomonori TSUKIYA**, Akihiko HOMMA**,
Tadayuki KAMIMURA**,***, Eisuke TATSUMI**,
Yoshiyuki TAENAKA** and Soichiro KITAMURA**

It has been conceived that the mechanical heart valves mounted in an artificial heart close much faster than in vivo use, resulting in cavitation bubbles formation. In this study, the mechanisms for cavitation in mechanical heart valves (MHVs) is investigated with monoleaflet and bileaflet valves in the mitral position with an electrohydraulic total artificial heart (EHTAH). The valve-closing velocity and pressure-drop through the valve were done, and a high-speed video camera was employed to investigate the mechanism for MHVs cavitation. The valve-closing velocity and pressure-drop of the bileaflet valves were less than that of the monoleaflet valves. Most of the cavitation bubbles in the monoleaflet valves were observed next to the edge of the valve stop and the inner side of the leaflet. With the bileaflet valves, cavitation bubbles were concentrated along the leaflet tip. Also, the number density of cavitation bubbles in the bileaflet valves was less than that of the monoleaflet valves. The number density of cavitation bubbles increased with an increase in the valve-closing velocity and the valve stop area. It is established that squeeze flow holds the key to cavitation in the mechanical heart valve. In a viewpoint of squeeze flow, the bileaflet valve with slow valve-closing velocity and small valve stop area, is safer to prevent of blood cell damage than the monoleaflet valves.

Key Words: Mechanical Heart Valve, Cavitation Bubble, Closing Velocity, Squeeze Flow

1. Inroduction

The cavitation phenomenon in mechanical heart valves is well documented and has been visualized by stroboscopic photography[1]-[3]. Cavitation in a liquid flow field occurs at locations where the local pressure falls below the vapor pressure of the liquid, creating vaporous bubbles in the field[4]. The collapse of the cavitation bubbles generates a high-speed micro-jet and shock waves that may damage the valve surface and blood components.

In general, the major causes of cavitation occurrence in a mechanical heart valve were as follows: venturi effect due to flow after valve closure at the narrow gap between leaflet and valve housing, water hammer effect due to the sudden stop of the MHV leaflets, and squeeze flow that can take place in the narrow gap between the closing leaflet and valve stop[5]. Bluestein et al.[6] reported that the caivtation bubbles cause to squeeze flow and its maximum velocity reach as high as 30 m/s. Lee et al.[7] and Shu et al.[8] examined the cavitation threshold of *dp/dt* for different mechanical heart valves using stroboscopic photography. He et al.[3] investigated the mechanism of the formation of cavitation bubbles in cases involving Medtronic Hall valves; in that study, the average value of the increase in the rate of transvalvular pressure was used as an index loading rate. However, the gradient of the ventricular pressure differed according to ventricular chamber compliance. In previous studies, we have shown that cavitation erosion on the valve surface increases with increases in the

* Received 21st May, 2004 (No. 04-4120)
** Department of Artificial Organs, Research Institute, National Cardiovascular Center, 5-7-1 Fujishiro-dai, Suita, Osaka 565-8565, Japan. E-mail: hslee@ri.ncvc.go.jp
*** Japan Association for the Advancement of Medical Equipment, 3-42-6 Hongo, Bunkyo-ku, Tokyo 113-0033, Japan

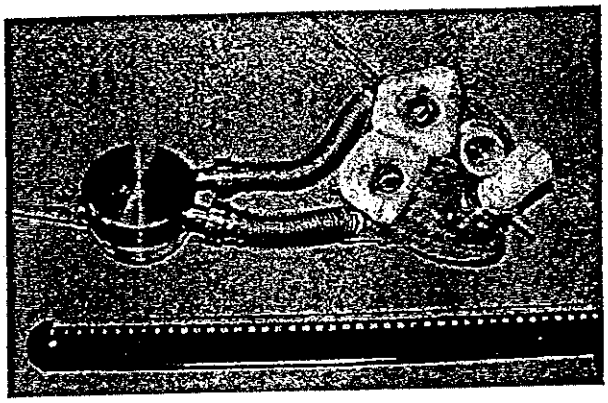

Fig. 1 An electrohydraulic total artificial heart

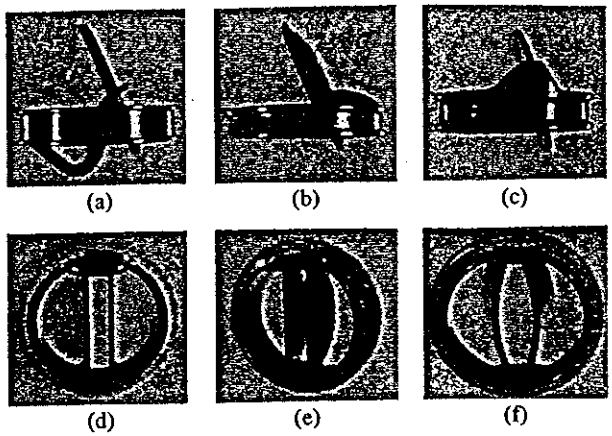

Fig. 2 Photographs of the mechanical heart valve (a) Medtronic Hall valve, (b) Björk-Shiley valve, (c) Omnicarbon valve, (d) St. Jude valve, (e) ATS valve, (f) Sorin valve

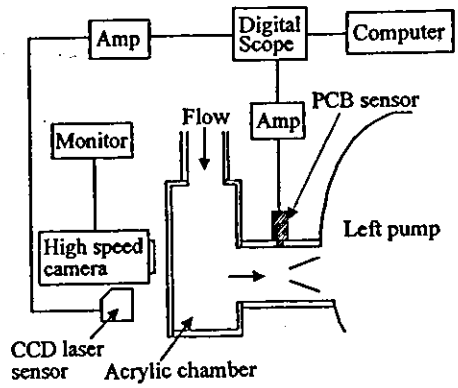

Fig. 3 Diagram of the experimental system

closing velocity[9),(10)]. Also, erosion pit generation due to cavitation has been shown to be restricted to an area on the valve surface next to the edge of the valve stop where the squeeze flow occurs.

Since 1987, our laboratory has been developing an electrohydraulic total artificial heart, and induced the mechanical heart valves[11),(12)]. Hemolysis was very important point in an electrohydraulic total artificial heart, which occurred by cavitation as well as shear stresses. We paid attention to cavitation phenomenon in MHV as a cause of the hemolysis, and to choice for the best mechanical heart valve in our EHTAH. In order to investigate the mechanisms for MHV cavitation with an electrohydraulic total artificial heart, the valve-closing velocity, pressure-drop measurements were done, and a high-speed video camera were employed.

2. Materials and Methods

The electrohydraulic total artificial heart (stroke volume: 80 mL) that was used in this study was developed by the National Cardiovascular Center in Japan (NCVC); this heart model consists of two diaphragm-type blood pumps, an actuator, and a controller (see Fig. 1)[11),(12)]. The actuator is connected to both blood pumps by a flexible tube. The flexible tubes are filled with silicon oil. This electrohydraulic total artificial heart system functions as follows: silicon oil drives the blood pump via the inverse and/or reverse rotation of the impeller. The electrohydraulic total artificial heart used in this study was connected to an overflow mock circulatory loop tester. Tap water at room temperature was used as a test fluid. In terms of pressure, the pre-and after-load of the right blood pump were fixed at 10 and 30 mmHg, respectively, and the pre-and after-load of the left blood pump were fixed at 10 and 100 mmHg, respectively.

The three kinds of the monoleaflet valves; a 25-mm Björk-Shiley valve, a 25-mm Medtronic Hall valve and a 23-mm Omnicarbon valve with opening angle of 70, 70 and 68°, respectively, and the three kinds of the bileaflet valves; a 21-mm St. Jude valve, a 21-mm ATS valve and a 21- mm Sorin valve with opening angle of 55, 60 and 60°, respectively, were used (see Fig. 2). Those various mechanical heart valves were mounted in the mitral position in an electrohydraulic total artificial heart. The mechanical heart valves were mounted on the rigid mounting; by inserting the valve in left blood pump housing made of polyurethane after removing the mechanical heart valve sewing ring.

A CCD laser displacement sensor (LC-2450, Keyence, Osaka) with a resonance frequency of 50 kHz was used to detect the closing motion of the leaflet just before closure (see Fig. 3). The chamber was constructed from acrylic resin for optical access, and the laser displacement sensor was placed on top of the acrylic chamber. A piezoelectric pressure transducer (105C02, PCB Piezotronics, Depew) with a resonant frequency of 250 kHz was mounted 10 mm away from the major orifice of the mitral valve surface (see Fig. 3). The mean value and standard deviation of the pressure drop and closing velocity were taken from the statistics of 30 times measurements. Then, to capture an image of the cavitation bubbles, a high-speed camera (fx-6000, nac, Tokyo) was used (see Fig. 3). The high-speed camera was

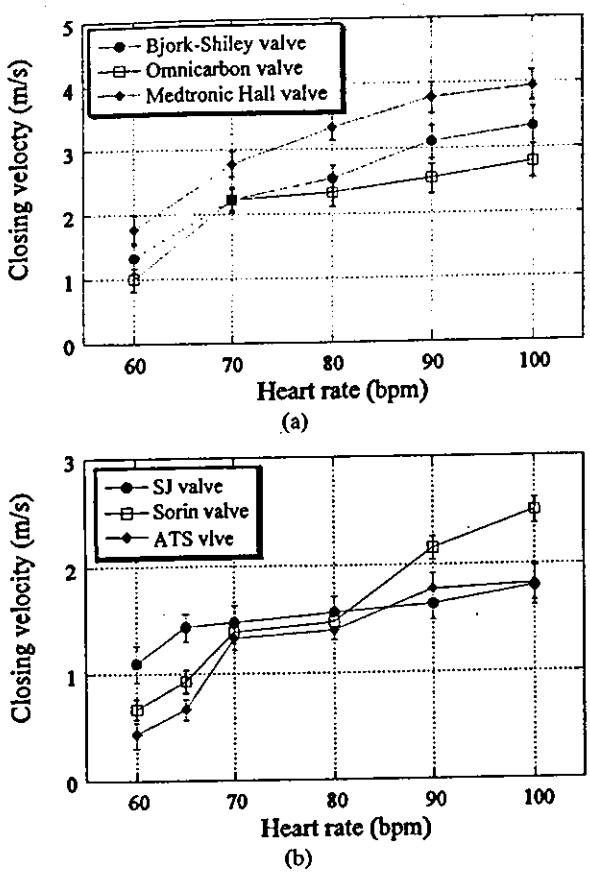

Fig. 4 The valve-closing velocity just before closure 0.3 ms (a) Monoleaflet valves, (b) Bileaflet valves

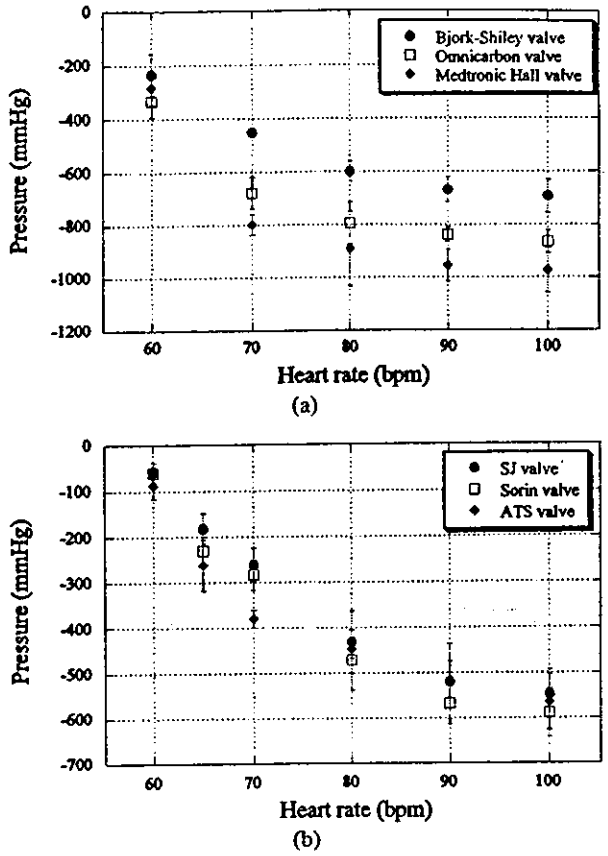

Fig. 5 The pressure-drop of the mechanical heart valve (a) Monoleaflet valves, (b) Bileaflet valves

placed on the top of the acrylic chamber; the behavior of the cavitation bubbles was recorded at 10 000 frames per second.

3. Results

Figure 4 shows the valve-closing velocity at 0.3 ms just before closure. The valve-closing velocity increased with an increase in the heart rate. The valve-closing velocity of the monoleaflet valves ranged from 1.0 to 4.0 m/s. Among the monoleaflet valves, valve-closing velocity of the Medtronic Hall valve was fastest. The bileaflet valve-closing velocity ranged from 0.5 to 2.5 m/s. With higher heart rate, the valve-closing velocity of the Sorin valve was greater than that of the other bileaflet valves.

The pressure-drop increased with an increase in the heart rate, its value of the bileaflet valves was significantly lower than those of the monoleaflet valves (see Fig. 5). Even with a higher heart rate, pressure-drop of the bileaflet valves did not reach a vapor pressure of –730 mmHg under atmospheric pressure at which tap water at 25°C come to a boil. On the other hand, the pressure-drop did reach a vapor pressure with the higher heart rate of the monoleaflet valves.

Images of cavitation in the monoleaflet valves at a heart rate of 70 bpm are shown in Fig. 6. Cavitation bubbles in the Medtronic Hall valve were observed next to the edge of the valve stop (see Fig. 6 (a)). With the Omnicarbon valve, cavitation bubbles were observed next to the edge of the valve stop and inner side of the leaflet (see Fig. 6 (b)). In the case of Björk-Shiley valve, cavitation bubbles were only observed on the inner side of the leaflet (see Fig. 6 (c)). Images of cavitation in the monoleaflet valves at a heart rate of 100 bpm are shown in Fig. 7. Cavitation bubbles in the Medtronic Hall valve and Omnicarbon valve were observed next to the edge of the valve stop and inner side of the leaflet (see Fig. 7 (a) and (b)). The area in which cavitation bubbles coved and the number density of bubbles generally increased with an increase of the valve-closing velocity.

Images of cavitation in the bileaflet valves at a heart rate of 70 and 100 bpm are shown in Figs. 8 and 9. Most of cavitation bubbles were concentrated along the leaflet tip, and the number density of bubbles increased with an increase of the valve-closing velocity.

4. Discussion

4.1 Water hammer effect

In mechanical heart valve, the pressure-drop due to water hammer was related to the valve-closing velocity. The valve-closing velocity increased with increas-

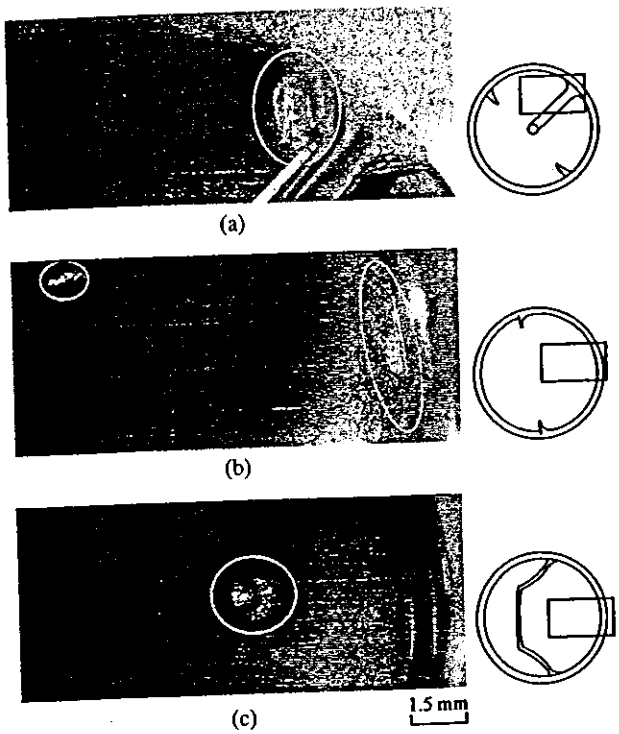

Fig. 6 Images of cavitation bubbles at a heart rate of 70 bpm (a) Medtronic Hall valve, (b) Omnicarbon valve, (c) Björk-Shiley valve

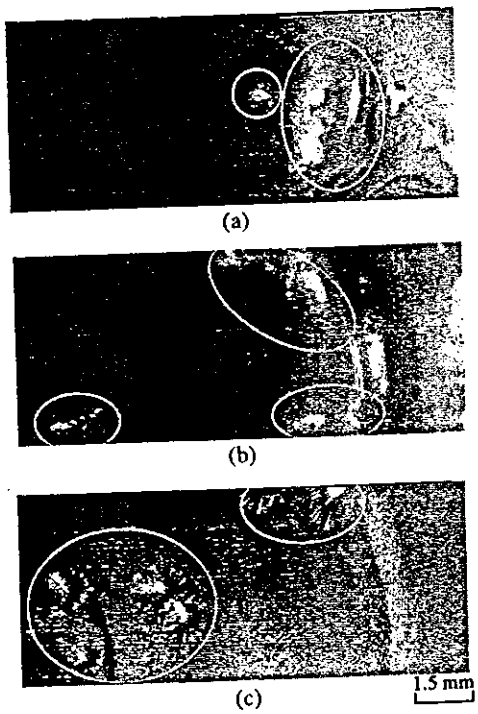

Fig. 7 Images of cavitation bubbles at a heart rate of 100 bpm when 200 μs after valve closure (a) Medtronic Hall valve, (b) Omnicarbon valve, (c) Björk-Shiley valve

ing the heart rate. With the higher heart rate, pressure-drop near the valve surface in the monoleaflet valves did reach the vapor pressure (−730 mmHg at 25°C), and cavitation bubble observed on the inner side of the leaflet of the monoleaflet valves (see Figs. 6 and 7). The cavitation bubble in the Björk-Shiley valve had a diameter of up to 1.5 mm, which cause water hammer effect.

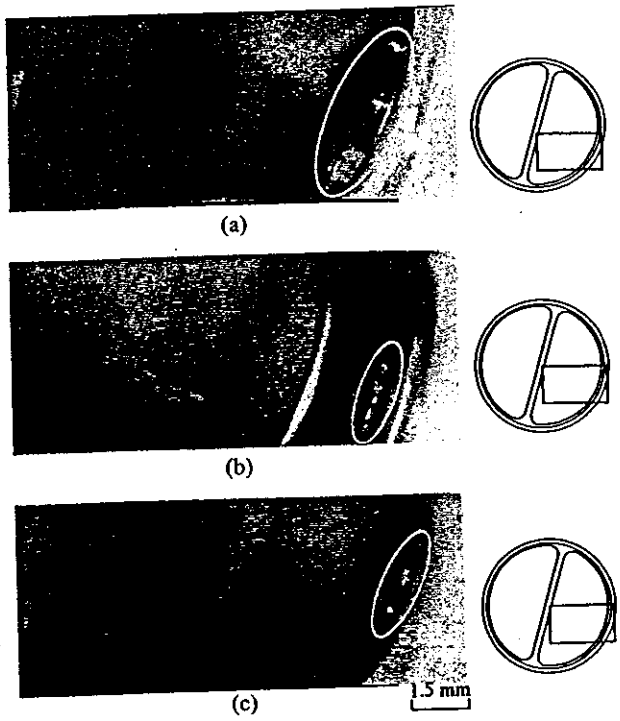

Fig. 8 Images of cavitation bubbles at a heart rate of 80 bpm when 200 μs after valve closure (a) St. Jude valve, (b) Sorin valve, (c) ATS valve

As shown in Fig. 4, the bileaflet valve-closing velocity was less than of the monoleaflet valves, because the moment arm is smaller, and that is the reason why the pressure-drop is smaller with the bileaflet valves (see Fig. 5). Therefore, even with a higher heart rate (see Fig. 5 (b)), pressure-drop of the bileaflet valves did not reach the vapor pressure, which related to not finding cavitation bubble at the inner side of the leaflet (see Figs. 8 and 9).

4.2 Squeeze flow

In all monoleaflet valves, most cavitation bubbles were observed next to the edge of the valve stop, which cause the squeeze flow between the leaflet and the valve stop. On the other hand, in the bileaflet valves, most of cavitation bubbles concentrated along the leaflet tip, which cause the squeeze flow.

The dynamics of fluid being squeezed through a narrow gap between the leaflet and the valve stop are accounted for by Reynold's equation. Assuming that the valve closes with a constant closing velocity (see Fig. 10), we can obtain from the narrow gap between the leaflet and the valve stop the following the Reynold's equation[13],

$$\frac{\partial}{\partial x}\left(h^3\frac{\partial p}{\partial x}\right)=-12\mu\frac{\partial h}{\partial t} \tag{1}$$

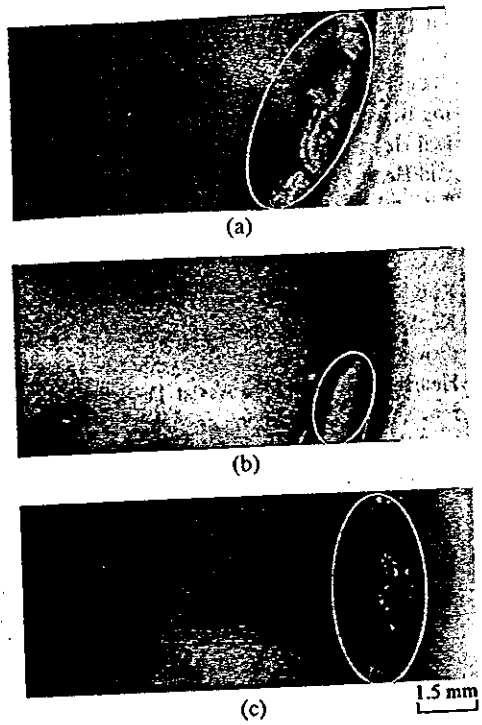

Fig. 9 Images of cavitation bubbles at a heart rate of 100 bpm when 200 μs after valve closure (a) St. Jude valve, (b) Sorin valve, (c) ATS valve

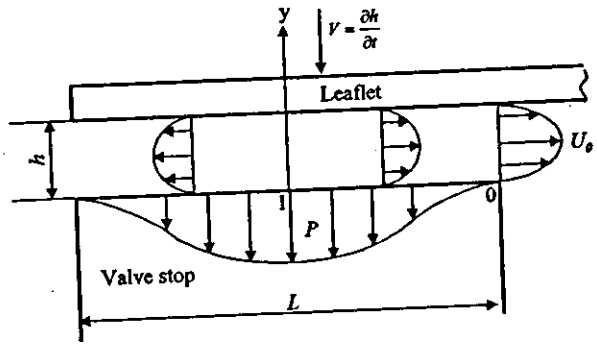

Fig. 10 A model of squeeze flow from a narrow gap between a leaflet and a valve stop. h, gap; L, the length of the valve stop; V, closing velocity of the leaflet

where h is the gap size and μ the fluid viscosity. From Eq. (1), we can define the following equation pressure distribution of the narrow gap between the leaflet and the valve stop center:

$$P - P_0 = \frac{12\mu}{h^3}\frac{\partial h}{\partial t}\frac{1}{2}\left\{\left(\frac{L}{2}\right)^2 - x^2\right\} \tag{2}$$

where L is the length of the valve stop, x is distance from the valve stop, and $\partial h/\partial t$ is the valve-closing velocity (see Fig. 10). Applying Bernoulli's equation to points 0 and 1 of Fig. 10, we can obtain the following equation:

$$P_1 + \frac{\rho U_1^2}{2} = P_0 + \frac{\rho U_0^2}{2} \tag{3}$$

where $U_1 = 0$, $P_0 = 0$; in addition, when substituting $x = 0$ for Eq. (2), we obtain P_1 of the pressure at point 1 (valve stop center) in Fig. 10:

$$P_1 = \frac{12\mu}{h^3}\frac{\partial h}{\partial t}\frac{L^2}{8} \tag{4}$$

By substituting Eq. (4) for Eq. (3), we can obtain the squeeze flow velocity from the valve stop U_0:

$$U_0 = \sqrt{\frac{3\mu}{4\rho h^3}\frac{\partial h}{\partial t}\cdot L^2} \tag{5}$$

where ρ is the density of the liquid. As shown in Eq. (5), the squeeze flow velocity is proportional to the valve-closing velocity, the area of the valve stop. Based on our results regarding squeeze flow, we conclude that slow valve-closing velocity and a small valve stop could minimize cavitation in mechanical heart valve.

From a viewpoint of squeeze flow, the bileaflet valve with less the number density of cavitation bubbles along the leaflet tip, assumedly preventing of blood cell damage than the monoleaflet valves. Although cavitation phenomenon in mechanical heart valves differs depending on the working fluid, the results of this study provide useful information on selecting the mechanical heart valve in an electrohydraulic total artificial heart.

5. Conclusions

The formation of cavitation bubbles depended on both the valve closing velocity and the valve leaflet geometry. Most of cavitation bubbles were observed at the contact point; the major cause of these cavitation bubbles was determined to be the squeeze flow. It is established that squeeze flow holds the key to estimate of MHV cavitation. The number density of cavitation bubbles cause by squeeze flow increased with an increasing the valve-closing velocity and the area of the valve stop. In the view point of squeeze flow, the bileaflet valves with slow closing velocity and a small valve stop area is better valve for our electrohydraulic total artificial heart.

Acknowledgements

This work was supported by foundation of Translational Research and New Energy and Industrial Technology Development Organization.

References

(1) Bachmann, C., Kini, V., Deutsch, S., Fontaine, A.A. and Tarbell, J.M., Mechanisms of Cavitation and the Formation of Stable Bubbles on the Björk-Shiley Monostrut Prosthetic Heart Valve, J. Heart Valve Dis., Vol.11 (2002), pp.105–113.

(2) Lin, H.Y., Bianccucci, B.A., Deutsch, S., Fontaine, A.A. and Tarbell, J.M., Observation and Quantification of Gas Bubble Formation on a Mechanical Heart Valve, Transactions of the ASME, Vol.122 (2000), pp.304–309.

(3) He, Z., Xi, B., Zhu, K. and Hwang, N.H.C., Mechanisms of Mechanical Heart Valve Cavitation: Investi-

gation Using a Tilting Disk Valve Model, J. Heart Valve Dis., Vol.10 (2001), pp.666–674.

(4) Knapp, R.T., Daily, J.W. and Hammitt, F.G., Cavitation, (1979), Institute of Hydraulic Research, University of Iowa.

(5) Garrison, L.A., Lamson, T.C., Deutsch, S., Geselowitz, D.B., Gaumond, R.P. and Tarbell, J.M., An in-Vitro Investigation of Prosthetic Heart Valve Cavitation in Blood, J. Heart Valve Dis., Vol.3(Suppl I) (1994), pp.S8–S24.

(6) Bluestein, D., Einav, S. and Hwang, N.H.C., A Squeeze Flow Phenomenon at the Closing of a Bileaflet Mechanical Heart Valve Prosthesis, J. Biomech., Vol.27, No.11 (1994), pp.1369–1378.

(7) Lee, C.S., Chandran, K.B. and Chen, L.D., Cavitation Dynamics of Mechanical Heart Valve Prostheses, Artif Organs, Vol.18 (1994), pp.758–767.

(8) Shu, M.C.S., Leuer, L.H., Armitage, T.L., Schneider, T.E. and Christiansen, D.R., In Vitro Observations of Mechanical Heart Valve Cavitation, J. Heart Valve Dis., Vol.3(Suppl. I) (1994), pp.S85–93.

(9) Lee, H.S., Tsukiya, T., Homma, A., Kamimura, T., Takewa, Y., Nishinaka, T., Tatsumi, E., Taenaka, Y., Takano, H. and Kitamura, S., Observation of Cavitation in a Mechanical Heart Valve in a Total Artificial Heart, ASAIO J., Vol.50 (2004), pp.205–210.

(10) Lee, H.S., Tsukiya, T., Homma, A., Taenaka, Y., Tatsumi, E. and Takano, H., Measurement of the Closing Behavior of the Björk-Shiley Monoleaflet Mechanical Heart Valve with an Electrohydraulic Total Artificial Heart, Artif Organs, Vol.27 (2003), pp.744–748.

(11) Tatsumi, E., Taenaka, Y., Homma, A., Nishinaka, T., Takewa, Y., Tsukiya, T., Ohnishi, H., Shirakawa, Y., Kakuta, Y., Shioya, K., Katagiri, N., Mizuno, T., Kamimura, T., Takano, H., Tsukahara, K., Tsuchimoto, K., Wakui, H. and Yamaguchi, H., The National Cardiovascular Center Electrohydraulic Total Artificial Heart and Ventricular Assist Device Systems: Current Status of Development, ASAIO J., Vol.49 (2003), pp.243–249.

(12) Tatsumi, E., Taenaka, Y., Uesho, K., Homma, A., Nishinaka, T., Kakuta, Y., Tsukiya, T., Takano, H., Masuzawa, T., Nakamura, M., Koshiji, K., Fukui, Y., Tsukahara, K., Tsuchimoto, K. and Wakui, H., Current Status of Development and in Vivo Evaluation of the National Cardiovascular Center Electrohydraulic Total Artificial Heart System, J. Artif Organs, (in Japanese), Vol.3 (2000), pp.62–69.

(13) Schlichting, H., Boundary Layer Theory, (1979), McGraw-Hill Book Co.